Journal of Physics Research (Hong Kong)
ISSN: 2789-9233 (print)
Shuangqing Academic Publishing House
http://www.qingpress.com

Superconducting Quantum Bits and Superconducting Quantum Computing

Feifan Su
Beijing National Laboratory for Condensed Matter Physics, Institute of Physics, Chinese Academy of Sciences, Beijing 100190, China

Abstract: With Google's successful demonstration of "quantum supremacy" in 2019, the research of superconducting quantum computing is attracting more and more attention around the globe. Superconducting quantum bits (qubits) are macroscopic devices with fundamental quantum properties such as energy-level quantization, quantum-state superposition, and quantum-state entanglement. They provide an excellent platform for studies in many fields such as quantum physics, atomic physics, quantum optics, quantum chemistry, quantum simulation, quantum computing, and so on. In this article, we will discuss the basic principles and structures of the superconducting phase-, charge-, transmon-, and flux-type qubits, as well as their device design and fabrication process. We will also present a brief introduction to the rich research areas based upon the superconducting qubit architecture.

Keywords: superconducting qubit, qubit fabrication, quantum-state measurement, quantum simulation, quantum computing

Between the 1970s and 1980s, the quantum properties such as macroscopic quantum tunneling, energy level quantization, resonant tunneling, photon induced transition and population inversion in Josephson junction and superconducting quantum interference device (SQUID) have attracted extensive interest of researchers [1,2]. At the turn of the 20th century, the research group of NEC in Japan successfully prepared the first superconducting qubit (charge qubit) by using the characteristics of Josephson junction. The test results showed the quantum coherent oscillation lasting about 2ns [3]. Shortly after that, Jonathan Friedman and John Martinis research group also successfully prepared superconducting qubits with different design structures. According to their design, they can be divided into phase qubits [4,5] and flux qubits [6]. Since then, the new qubits developed can be regarded as the deformation of the above three types of qubits. The coherence time of a quantum system is the "lifetime" of the system, and a long coherence time is the necessary

---

Article history: Received Nov 29, 2021 Accepted Jan 18, 2022 Available online Jan 24, 2022
To cite this paper: Feifan Su(2022). Superconducting Quantum Bits and Superconducting Quantum Computing. Journal of Physics Research (Hong Kong), Vol2, Issue1, Pages 1-18.

basis for superconducting qubits to participate in quantum physics research and quantum computing. The "Moore's law" of superconducting qubits proposed in 2018 [7], which points out that the decoherence time of superconducting qubits has increased by an order of magnitude in almost five years. After near 20 years of continuous efforts in device design, materials, fabrication technology and measurement methods, the decoherence time of superconducting qubits has made great progress by increased 100000 times [8]. And various research groups have significantly expanded the number of qubits with quantum entanglement in the form of coupled superconducting qubits. In 2019, the number of qubits on Google's "sycamore" qubit chip has reached 54 [9]. These advances have laid an effective foundation for subsequent research. The quantum computing platform built by superconducting circuits and qubits can study and simulate many scientific problems such as quantum physics, atomic physics, quantum optics, quantum chemistry [10-19]. It is precise because superconducting quantum computing has the characteristics of easy expansion of the number of qubits, good compatibility with mature microwave systems, convenient preparation of quantum states, and wide space for improving the decoherence time of samples. Therefore, superconducting quantum bits have become one of the most promising schemes to realize general quantum computing.

This paper mainly introduces the basic principles and structural composition of different types superconducting qubits, the preparation technology and quantum state measurement technology of superconducting qubits, and the research content of specific problems using superconducting qubits, so clarify the general principles and methods of superconducting quantum bits and superconducting quantum computing.

1. SUPERCONDUCTING QUANTUM CIRCUITS AND QUBITS

The circuit on the superconducting qubit chip is a superconducting circuit under normal working conditions, and the elements of superconducting circuits can be regarded as two categories. Common elements are consistent with general circuits, including capacitors, inductors and resistors; however, the core element is Josephson junction and resonator. To understand the working principle of superconducting qubits, first understand the macro quantum phenomenon principle of Josephson junction. According to the BCS theory of superconductors [20], the electrons in the superconductor will form a Cooper pair with charge $2e$, mass $2m_e$ and spin is zero, and the state can be described by wave function $\psi(r,t)$.We need to pay close attention to two superconductor properties. The first point is the quantization of magnetic flux. When a closed loop ring with a magnetic field reaches the temperature below the superconducting transition temperature, if the magnetic field is removed at this time, the magnetic flux generated by the superfluid in the closed loop ring is quantized. The flux quantum is $\varphi_0 = h/2e \approx 2.07\times10^{-15}\ \mathrm{Tm}^2$, The nature of flux quantization requires that the wave function is a single value wave function $\psi(r,t)$. The second point is the Josephson tunnel effect. Josephson junction comprises two superconductors layers with a 2 ~ 3 nm insulating layer. Cooper pairs can maintain coherence when tunneling through the insulating layer. The supercurrent I passing through the insulating barriergauge and the invariant phase difference between two superconductors are satisfies the Josephson equation

$$I = I_c \sin\delta\ ,\ \frac{h}{2\pi}\frac{d\delta}{dt} = 2eV \quad (1)$$

Where I_c is the critical current of Josephson junction, V is the potential difference at both ends of Josephson junction and Planck constant h.

It can be seen from formula (1) that Josephson junction is a non dissipative device with nonlinear inductance $|L_J| = \phi_0/(2\pi I_c\cos\delta)$, it is the key property of superconducting qubits. Therefore, the Josephson junction can be equivalent to the RCSJ model circuit structure[21] as shown in Fig. 1 (a), in this model, Josephson junction is equivalent to three parts: capacitance, inductance and superconducting current. The model can be written by Kirchhoff's law as

$$I_{\mathrm{tot}} = I + C\,dV/dt + V/R$$

Further, the dynamic equation of the system can be obtained

$$m\frac{d^2\delta}{dt^2} + \frac{m}{RC}\frac{d\delta}{dt} = -\frac{\partial U(\delta)}{\partial\delta} \qquad (2)$$

Where $m = (\phi_0/2\pi)^2 C$ is the mass of the system quasiparticle and $U(\delta) = -E_J(\frac{I_{tot}}{I_c}\delta + \cos\delta)$, $E_J = \frac{\phi_0}{2\pi} I_c$ is the Josephson energy. Therefore, the Hamiltonian of the system can be written as

$H = \dfrac{Q^2}{2C} + U(\delta), Q = 2en$, n is the Cooper logarithm operator.

In this way, $U(\delta) = -E_J(\dfrac{I_{tot}}{I_c}\delta + \cos\delta)$ can be understood as the system potential energy term as shown in Fig. 1 (b). Generally, because the potential energy curve is similar to a washboard, this potential energy is also called "washboard potential". With the above foundation, it can be seen that the height and energy level spacing of the washboard barrier can be controlled by controlling the current I_{tot}. When $I_{tot}/I_c \geqslant 1$, the potential well disappears. At this time, it can be vividly understood that the quasi particle will move downward along the potential energy curve. According to Josephson equation, there will be potential difference at Josephson junction, and $I_{tot}/I_c < 1$ the potential well is existential, the quasi particle is in the potential well, and there is no potential difference at Josephson junction. Moreover, when the potential well is shallow, the quasi particle will have a certain probability of tunneling out of the potential well. The Josephson junction will change from zero potential difference to nonzero potential difference. In this way, Josephson junction can show detectable "quantum" in the macroscopic.

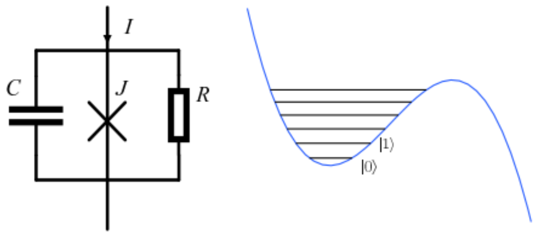

(a) RCSJ model of Josephson junction (b) washboard potential curve

Figure 1. RCSJ model and its potential energy curve

1.1 PHASE QUBIT

The phase qubit can be regarded as a current biased Josephson junction, if the lowest two energy levels in the washboard potential well are regarded as the $|0\rangle$ state and $|1\rangle$ state of qubits (similar to the 0 and 1 of classical computers). When the potential barrier is high enough, the phase qubit can be initialized by microwave pulse regulation. Next, adjust the appropriate barrier height so that the quasi particles can tunnel out of the potential well. According to the above discussion, the quantum state of the system can be read out by measuring the potential difference at the Josephson junction superconductor.

In addition to the control current I_{tot} to control the height and energy level spacing of the washboard barrier, in order to reduce the influence of the noise introduced by the bias current on the phase qubit, the magnetic flux ϕ can also be used as an experimental controllable parameter in conjunction with RF SQUID[5]. As shown in Fig. 2, the equation corresponding to this design structure can be written as

$$m\frac{d^2\Phi}{dt^2}+\frac{m}{RC}\frac{d\Phi}{dt}=-\frac{\partial U(\Phi)}{\partial \Phi} \quad (3)$$

Where ϕ_e is the applied magnetic flux, $\Phi=\phi_{tot}/\phi_0$,

$$U(\phi)=\frac{\phi_0}{2L}\left[(\frac{\phi_{tot}}{\phi_0}-\frac{\phi_e}{\phi_0})^2-\frac{\beta_L}{2\pi^2}\cos(2\pi\frac{\phi_{tot}}{\phi_0})\right],\ m=\phi_0^2C,\ \beta_L=2\pi LI_c/\phi_0\ (L \text{ is loop inductance})$$

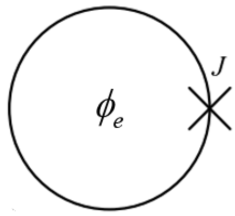

Figure 2. Schematic diagram of RF SQUID phase qubit structure with magnetic flux bias

In the experiment, $1<\beta_L<3.5$ is generally required to make the potential well in the form of double well as shown in Fig. 3. At this time, the potential barrier of the potential well can be increased or reduced by changing the external magnetic flux ϕ_e in the coil, and then the energy level suitable for the measurement system can be selected as the two states of the qubit[22-25].

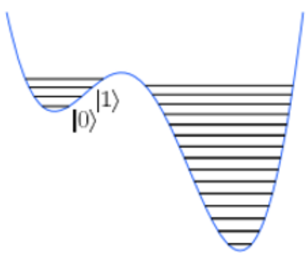

Figure 3. potential well and energy level of RF SQUID phase qubit

The optical microscope photo of RF SQUID type phase qubit fabrication by multilayer process[26] is shown in Fig. 4. The design of the device is similar to UCSB design[24]. The SQUID in this design includes three Josephson junctions, one small junction is connected in series with two large ones, and the critical current of the large junction is 1.7 times that of the small junction, the advantage of this design is that there is no need to measure the external magnetic flux separately ϕ_e.

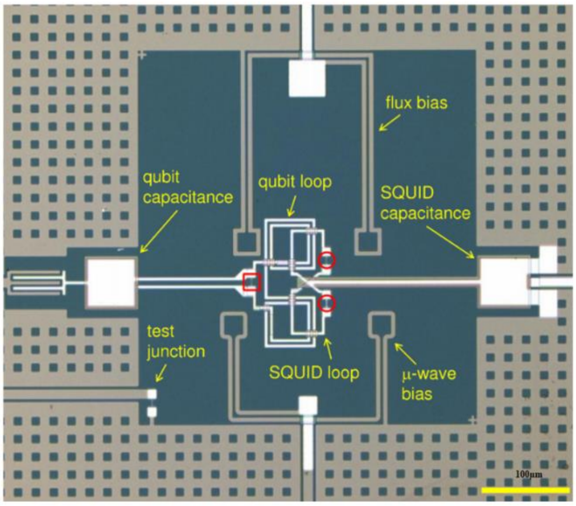

Figure 4. optical photo of RF SQUID type phase qubit. The positions of red box and circle are the qubit and Josephson junction of squid detector respectively[26]

1.2 CHARGE QUBIT AND TRANSMON QUBIT

Charge qubit is the earliest qubit design in history[3], and its design diagram is shown in Fig. 5. A gate capacitor C_g is connected in series with a Josephson junction, biased by the gate voltage V_g.

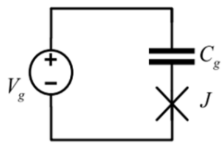

Figure 5. Schematic diagram of voltage biased superconducting charge qubit structure

The Hamiltonian of the system is

$$H = (Q - C_g V_g)^2 / 2(C + C_g) - E_J \cos\delta$$

Where $Q = 2en$ is the total charge in the gate capacitance and Josephson junction capacitance. If the Hamiltonian is expressed by the number of charges, it can be written as

$$H = 4E_C(n-n_g)^2 - E_J\cos\delta \quad (4)$$

Where n is the number of Cooper pairs, $n_g = C_gV_g/2e$ and $E_C = e^2/2(C+C_g)$ is the charge energy. The charge qubit works in the region where the E_J/E_C is far less than 1 so charge energy dominates. Fig. 6(a) is the energy spectrum of the charge qubit when $E_J/E_C = 0.2$.

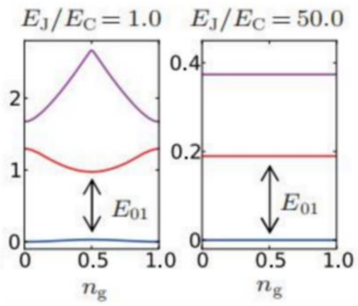

Figure 6. (a) Charge qubit energy spectrum at $E_J/E_C = 1.0$, (b) Charge qubit energy spectrum at $E_J/E_C = 50$

It can be seen that the energy level of charge qubit will change periodically with the change of n. Nakamura's research group observed coherent quantum oscillation of ns order for the first time[3]. In areas where E_J/E_C far greater than 1 so Josephson energy E_J can dominate. As shown in Fig. 6(b) ($E_J/E_C = 50$), at this time, the energy spectrum is flat and the spacing of each energy level does not change periodically with the number of charges n, at this time, the qubit is not sensitive to charge noise, which will undoubtedly improve the coherence time of the qubit. In the experiment, the lowest two energy levels in the potential well of the transmon qubit shown in Fig. 7 can be selected as the state $|0\rangle$ and the state $|1\rangle$. The transmon qubit is the improved design of the charge qubit using the above considerations[27-29]. Compared with the charge qubit, the transmon qubit has a qualitative improvement in coherence time. At present, the coherence time of transmission sub qubits is mostly 30-50 μs.

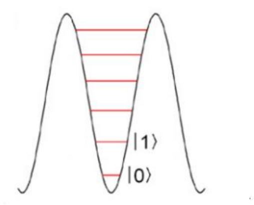

Figure 7. Potential well and energy level of transmission quantum bit

Experimentally, the transmon qubit can be designed by connecting the capacitor and Josephson junction in parallel and biased by the gate voltage V_g. The transmon qubit [30] in the 3D cavity is shown in Fig. 8 (a). The amplification part is the qubit with Josephson junction in the center. One side of the two large pads is the capacitor electrode, and the other side is used to read the qubit like coupling resonator. In addition, the resonator can also protect the qubit from the electromagnetic noise of the external environment. The transmon qubit in this 3D cavity has good performance with energy relaxation time T_1 = 60 μs and coherence time T_2 = 20 μs. The picture of 2D transmission sub qubit[31] is shown in Fig. 8 (b), in which the two large plates are the two electrodes of the capacitor, the Josephson junction is located in the central position between the electrode plates of the central capacitor, the two smaller plates at the bottom are used for the capacitive coupling between the qubit and other qubits, and the measurement of qubit state depends on the small plate at the top of the figure, although the 2D transmon qubit is slightly inferior to the 3D transmon qubit, the energy relaxation time can reach T_1 = 30 μs and the coherence time can reach T_2 = 20 μs.

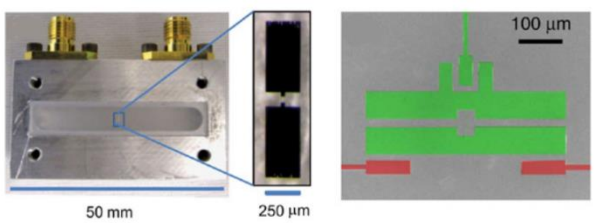

(a) 3D transmission sub qubit optical photo [30] (b) 2D transmission sub qubit optical photo [31]

Figure 8. 3D and 2D transmon qubit

Xmon qubit is an optimized design of transmon qubit by John Martinis's research group of UCSB [33]. The center of Xmon qubit is a cross capacitor structure, and the single Josephson junction in transmon qubit is replaced by double junction design. This design makes it easier for adjusted and read out the state of Xmon qubits by the coupled readout resonator (discussed in detail later), and it is also easier to be coupled with other qubits or other subsequent required resonators, so it can be simply expanded in the number of qubits.

As shown in Fig. 9, the four arms of the Xmon qubit cross structure are respectively connected to XY control, Z control, capacitive coupling with other qubits and resonant cavity for qubit state readout. At present, the reported energy relaxation time of Xmon qubit is 40 μs on average. This design's scalability and excellent coherence time make Xmon qubit the most common superconducting qubit in various studies.

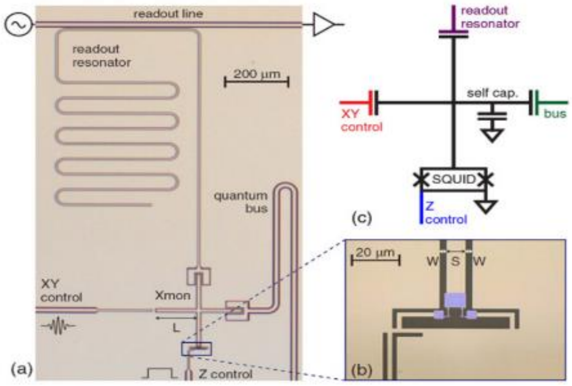

Figure 9. Xmon qubit optical photo, xmon qubit equivalent circuit structure diagram and Josephson junction optical photo [33] (purple part in the figure)

1.3 FLUX QUBIT

Mooij proposed the design of flux qubit in 1999[34]. As shown in Fig 10, it is composed of superconducting rings composed of three Josephson junctions. One of the three Josephson junctions is α times smaller than the other two junctions. In this design, Josephson provides a larger inductance, and the inductance of the small loop connected in parallel with the smaller Josephson junction capacitor can be ignored, which makes it less sensitive to external noise. Since each Josephson junction has a washboard potential, the potential energy of the flux qubit is in a two-dimensional[35] form as shown in Fig. 11, the expression is

$$U(\delta_1,\delta_2)=E_J(2-\cos\delta_1-\cos\delta_2)+\alpha E_J[1-\cos(2\pi f+\delta_1-\delta_2)] \quad (5)$$

Where δ_1 and δ_2 is the phase difference of two large junctions, δ_3 is the phase difference of small junctions, $2\pi f=-(\delta_1-\delta_2+\delta_3)$.

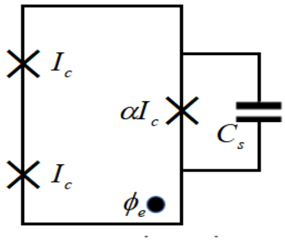

Figure 10. Schematic diagram of magnetic flux qubit

The double well potential energy curve shown in Fig. 12 is the part intercepted along the red line segment in Fig. 12. The height of the two-part vertical potential well can be adjusted by α changing. Generally, the value of α is in the range of 0.5-0.7 or less than 0.5. In this range, quasi particles at two energy levels are more likely to tunnel under the condition of external magnetic flux $\phi_e = \phi_0/2$. Because $|0\rangle$ and $|1\rangle$ correspond to the current in the opposite direction in the flux qubit ring, the two states of qubit can be easily detected in experiment.

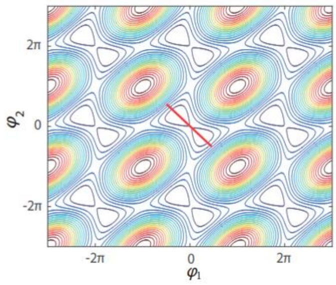

Figure 11. Contour plot of two-dimensional potential described by formula (5)

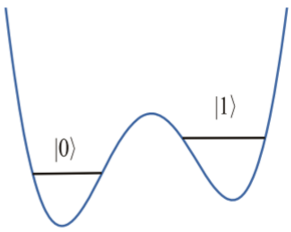

Figure 12. The potential well and energy level along the direction indicated by the red line in Fig. 11 when $\phi_e = \phi_0/2$ (the state in the two potential wells corresponds to the current in the opposite direction in the qubit ring)

Further research shows that the coherence time of flux qubit depends on the value of α strongly[36], when its value below 0.5, the characteristic of flux qubit with double potential wells will weaken with the decrease of barrier height, and the flux qubit will have a potential well shape similar to that of transmon qubit. Through this way, the energy relaxation time of flux qubit can reach 80 μs[37]. In addition, more research reports show that the performance of flux qubits still can improve[38]. Reviewing the development of superconducting qubits, the earliest charge qubits have only ns coherence time, while the transmon qubits improved from charge qubits eliminate the influence of charge noise, so as to eliminate the main source of decoherence, and increasing the coherence time of qubits to the order of 100 μs. Moreover, the design structure of the transmon qubit is simple, and the fabrication process is greatly simplified compared with the early phase qubit. In addition, in the past decade, people have studied the dielectric loss of the two-dimensional resonator and the methods to improve the performance of the qubit in detail[39-49]. These factors make people confident that the coherent time can reach the order of ms, the number of entangled qubits can reach more than 100, and the qubit chip with very high fidelity can be realized in the near future.

2. THE FABRICATION OF SUPERCONDUCTING QUBITS

The fabrication process of qubit is similar to that of the semiconductor chip, which can be roughly divided into three parts: layout design, streaming, packaging, and testing. However, in order to realize high-performance qubit devices, detailed research and exploration need to be carried out in the aspects such as fabrication process, substrate material pretreatment and device material selection. At present, the mainstream fabrication process route is to grow metal aluminum film on sapphire substrate, then use lithography and metal etching process to transfer the design pattern to prepare superconducting circuit, and use metal aluminum double angle evaporation method to prepare Josephson junction meeting the device design requirements at the designated position of superconducting circuit. Finally, the prepared qubits are rechecked and tested then cutting and ultrasonic spot welding package.

In the summary report [50] issued by John Martinis's research group in 2014, the key properties such as dielectric loss and additional inductance on the substrate material are described in detail, the energy loss mechanism of Josephson junction and the energy loss of superconducting circuit on chip are systematically studied. In recent years, research on the pretreatment methods of substrate materials shows that the cleanliness of substrate materials is directly related to the decoherence time of qubits[51]. The coherence time of qubit has been improved to varying degrees by pretreat sapphire substrates with "piranha" solution, annealed at high temperature[52] and high ancestral silicon substrates. In addition, some new metal materials, such as metal niobium and tantalum, also show their unique advantages in replacing metal aluminum to prepare quantum bits for superconducting circuits. The energy relaxation time of Xmon qubit prepared by these new processes and materials can reach 0.3ms[51], the superconducting quantum computing auxiliary Josephson parameter amplifier prepared by these new material processes can achieve an effective amplification frequency range of 600MHz, gain of 20dB and noise level close to the quantum limit in an extremely low temperature environment of 10mk[53].

3. QUANTUM NONDESTRUCTIVE MEASUREMENT

Fast and accurate reading of qubit states is the basis of superconducting quantum computing. At present, the measurement scheme widely used by various research units groups is quantum non-destructive measurement (QND) technology based on circuit cavity quantum electrodynamics (CQED) structure[54-56]. Compared with the scheme of detecting quantum states using DC SQUID, quantum non-destructive measurement based on CQED has many advantages. The most significant advantage is that QND does not destroy the quantum states of qubits and significantly improves the measurement rate. After continuous development, this technology can be used for the measurement of phase qubit[57], flux qubit[58-60] and the special transmon qubit.

In QED system, qubits are coupled with resonators, and the Hamiltonian of the coupling system is Jaynes Cummings form

$$H = \eta\omega_r(a^+a+1/2)+(\eta\omega_q/2)\sigma^z+\eta g(a^+\sigma^- +\sigma^+a) \quad (6)$$

Where ω_r, ω_q, g are the resonant cavity frequency, the quantum bit transition frequency and the coupling strength between the quantum bit and the resonant cavity, a^+ and a are photon generation and annihilation operators, $\sigma^\pm = (\sigma^x \pm i\sigma^y)/2$ is qubit transition operator based on common Pauli matrix after ignoring intracavity loss. The detuning between the frequency of qubit and the frequency of resonant cavity $\Delta = \omega_q - \omega_r$, the coupling g are two key parameters in Hamiltonian, When $\Delta = 0$, photons are exchanged between the resonant cavity and the qubit, the interaction between them will cause n degenerate energy levels to split with a width of $2g\sqrt{n}$. In the dispersion state ($\Delta >> g$), the frequency detuning between the resonator, as a result, photons are no longer exchanged directly, and the energy levels of the resonator and the qubit are mutually exclusive. In this case, by unitary transformation and taking the second-order approximation of g, the Jaynes Cummings Hamiltonian can be written as

$$H' = \eta\,(\omega_r + \chi\sigma_z)\, a^{+}a + [\eta\,(\omega_q + \chi)\,\sigma_z]/2 \qquad (7)$$

Where $\chi = g^2/\Delta$ is dispersion displacement and represents the frequency shift associated with the quantum state. The above Hamiltonian shows that the resonant frequency of the resonator is affected by the state of qubit, when the qubit is in the $|0\rangle$ state, the resonant frequency of the resonator is $\omega_r + \chi$, when the qubit is in $|1\rangle$ state, the resonant frequency of the cavity is $\omega_r - \chi$. In this way, we can detect the state of qubits according to the resonant cavity. Any change in photons number in the resonator will change the frequency and phase of qubits, so the fluctuation of the number of photons in the resonator should be reduced as much as possible. Experiments show that the non-destructive measurement of qubit quantum states can be realized when the microwave power is low, ensuring that the average number of photons in the resonant cavity is small[54]. The combination of high performance, most purpose qubits and efficient measurement methods has laid a foundation for superconducting quantum computing based on superconducting qubits, making new progress in superconducting quantum computing.

4. EXPERIMENTAL RESEARCH BASED ON SUPERCONDUCTING QUBIT

Superconducting circuits and superconducting qubits provide a good hardware tool for the study of quantum physics, atomic physics and quantum optics because of macro quantum effects, easy control of system parameters, convenient preparation and scalability. In the quantum simulation experiment by superconducting qubit, the Hamiltonian of the simulated quantum system can be directly mapped to the Hamiltonian of the superconducting qubit system. Therefore, superconducting quantum simulation based on superconducting qubits has natural advantages over classical computers in the research of quantum physics, quantum chemistry, condensed matter physics, cosmology and high energy physics. In recent years, superconducting qubits have been used to study the resonance escape and bifurcation of nonlinear systems under strong driving in quantum optics[61,62], macroscopic quantum tunneling in cuprate materials and quantum states phase diffusion in condensed matter physics[63,64], quantum random synchronization in dissipative quantum systems[65], topological phase diagrams and phase transitions of interacting quantum systems[66], Schrödinger cat state[67], Autler Townships splitting phenomenon in quantum optics[67-70], coherent group transfer in stimulated Raman adiabatic channels[12], electromagnetically induced transparency[71,72], resonance fluorescence and correlation emission laser[73,74].

Of course, the ultimate goal of quantum computing is to realize the general quantum computer. As early as the 1980s, American physicist Richard Feynman put forward the concept of quantum computer[75], in the mid-1990s, Shor and Grover proposed two quantum factor decomposition algorithms[76] and quantum search algorithms[77] respectively, which show that quantum computers have absolute advantages over classical computers in computing power. In 2019, Google announced the realization of quantum supremacy[9], which indicates that the general quantum computer is getting more closer to us. At present, superconducting quantum computing based on superconducting qubits, together with other quantum computing schemes[78-84], has become a powerful tool for many scientists who continue to explore the physical world to pursue their common ideals[85].

REFERENCE

[1] Devoret M H, Esteve D, Urbina C, et al.2002 in Exploring the quantum classical frontier: Recent advances in macroscopic phenomena Friedman J R and Han Siyuan eds[J]. (New York: Nova Science Publishers).

[2] Han Siyuan 2002 in Exploring the quantum classical frontier: Recent advances in macroscopic phenomena Friedman J R and Han Siyuan eds[J]. (New York: Nova Science Publishers) .

[3] Nakamura Y, Pashkin Y A and Tsai J S[J] 1999 Nature 398 6730.

[4] Martinis John M, Nam S, Aumentado J, et al[J]. 2002 Phys. Rev. Lett. 89 117901.

[5] Yu Yang, Han Siyuan, Chu Xi, et al[J] 2002 Science 296 889.

[6] Friedman, J. R., Patel, V., Chen, et al. Quantum superpositions of distinct macroscopic states[J]. Nature 406, 43–46 (2000).

[7] Oliver W D. Quantum engineering of superconducting qubits [J]. GoogleTechTalks: https://www youtube com/watch, 2018.

[8] Hover D, Zhu S, Thoreck T, et al. High fidelity qubit readout with the superconducting low-inductance undulatory galvanometer microwave amplifier [J]. Applied Physics Letters, 2014, 104(15): 152601

[9] J.M.Martinis. Nature 2019 574.

[10] Y. Makhlin, G. SchoN, A. Shnirman. Quantum-state engineering with josephson-junction devices[J]. Physics 73, 357–400 (2007).

[11] H. Paik, et al. Observation of high coherence in josephson junction qubits measured in a three-dimensional circuit QED architecture[J]. Phys. Rev. Lett. 107, 240501 (2011).

[12] H. K. Xu, C. Song, W. Y. Liu, et al, Coherent population transfer between uncoupled or weakly coupled states in ladder-type superconducting qutrits[J]. Nature Communications, volume, 7, 11018 (2016).

[13] Makhlin Y, Schon G and Shnirman A[J] 2001 Rev. Mod. Phys. 73 357.

[14] Wendin G and Shumeiko V S 2006 in Handbook of Theoretical and Computational Nanotechnology Rieth M and Schommers W eds[M]. (American Scientifific Publishers)

[15] Clarke J and Wilhelm F K[J]. 2008 Nature 453 1031.

[16] You J Q and Nori F[J]. 2011 Nature 474 589.

[17] Devoret M H and Schoelkopf R J[J] 2013 Science 339 1169.

[18] Georgescu I M, Ashhab S and Nori F[J] 2014 Rev. Mod. Phys. 86 153.

[19] Tinkham M 1996 Introduction to Superconductivity [J] (New York: McGraw-Hill).

[20] Bardeen, J., Cooper, L. N. & Schrieffer, J. R. Theory of superconductivity[J]. Phys. Rev.108, 1175–1204 (1957).

[21] M.Tinkham. Introduction to superconductivity[J] (New York:McGraw-Hill) (1996).

[22] Simmonds R W, Lang K M, Hite D A, et al[J]. 2004 Phys. Rev.Lett. 93 077003.

[23] Martinis J M, Cooper K B, McDermott R, et al[J]. 2005 Phys. Rev. Let. 95 210503.

[24] Neeley M, Ansmann M, Bialczak R C, et al[J]. 2008 Phys. Rev. B 77 180508.

[25] Martinis J M 2009 Quantum Inf. Process. 8 81.

[26] Su F F, Liu W Y, Xu H K, et al[J]. 2017 Chin. Phys. B 26 060308.

[27] Koch J, Yu T M, Gambetta J, et al[J]. 2007 Phys. Rev. A 76 042319.

[28] Houck A A, Schuster D I, Gambetta J M, et al[J] 2007 Nature 449 328.

[29] Majer J, Chow J M, Gambetta J M, et al[J]. 2007 Nature 449 443.

[30] Paik H, Schuster D I, Bishop L S, et al. 2011 Phys. Rev. Lett[J]. 107 240501.

[31] Chow J M, Gambetta J M, Magesan E, et al[J]. 2014 Nat. Commun. 5 4015.

[32] C ́orcoles A D, Magesan E, Srinivasan S J, et al[J]. 2015 Nat. Commun. 6 6979.

[33] Barends R, Kelly J, Megrant A, Sank D, et al[J]. 2013 Phys. Rev. Lett. 111 080502.

[34] Mooij J E, Orlando T P, Levitov L, et al[J]. 1999 Science 285 1036.

[35] T. P. Orlando, et al. Superconducting persistent-current qubit[J]. Physical Review B 60, 15398–15413 (1999).

[36] Steffen M, Kumar S, DiVincenzo D P, et al[J]. 2010 Phys. Rev. Lett. 105 100502.

[37] Yan F, Gustavsson S, Kamal A, et al[J]. 2016 Nat. Commun. 7 12964.

[38] Gustavsson S, Yan F, Catelani G, et al[J]. 2016 Science 354 1573.

[39] Gao J, Daa M, Vayonakis A, et al[J]. 2008 Appl. Phys. Lett. 92 152505.

[40] Wang H, Hofheinz M, Wenner J, et al[J]. 2009 Appl. Phys. Lett. 95 233508.

[41] Barends R, Vercruyssen N, Endo A, et al[J]. 2010 Appl. Phys. Lett. 97 023508.

[42] Wenner J, Barends R, Bialczak R C, C et al[J]. 2011 Appl. Phys. Lett. 99 113513.

[43] Sage Jeremy M, Bolkhovsky Vladimir, Oliver William D, et al[J]. 2011 J. Appl. Phys. 109 063915.

[44] Megrant A, Neill C, Barends R, et al[J]. 2012 Appl. Phys. Lett. 100 113510.

[45] Geerlings K, Shankar S, Edwards E, et al[J]. 2012 Appl. Phys. Lett. 100 192601.

[46] Chang J B, Vissers M R, C ́orcoles A D, et al[J]. 2013 Appl. Phys. Lett. 103 012602.

[47] Quintana C M, Megrant A, Chen Z, et al[J]. 2014 Appl. Phys. Lett. 105 062601.

[48] Bruno A, de Lange G, Asaad S, et al[J]. 2015 Appl. Phys. Lett. 106 182601.

[49] Gambetta J M, Murray C E, Fung Y K K, et al[J]. 2017 IEEE Trans. Appl. Supercond. 27 1700205.

[50] Martinis J M, MEGRANT A. UCSB final report for the CSQ program: Review of decoherence and materials physics for superconducting qubits[J]. arXiv preprint arXiv:14105793, 2014.

[51] Alex P. M. Place, Lila V. H. Rodgers, Pranav Mundada, et al[J]. arXiv preprint arXiv:2003.00024v1 2020.

[52] Megrant A, Neill C, Barends R, et al. Planar superconducting resonators with internal quality factors above one million [J]. Applied Physics Letters, 2012, 100(11): 113510.

[53] Su Feifan, Wang Ziting, Xu Huikai, et al. Nb-based Josephson parametric amplifier for superconducting qubit measurement[J]. Chinese Physics B, 2019, 28(11):110303.

[54] Blais A, Huang R S, Wallraff A, et al[J]. 2004 Phys. Rev. A 69 062320.

[55] Wallraff A, Schuster D I, Blais A, F et al[J]. 2004 Nature 431 162.

[56] Gambetta J, Blais A, Schuster D I, et al[J]. 2006 Phys. Rev. A 74 042318.

[57] Whittaker J D, da Silva F C S, Allman M S, et al[J]. 2014 Phys. Rev. B 90 024513.

[58] Lupascu A, Verwijs C J M, Schouten R N, et al[J]. 2004 Phys. Rev. Lett. 93 177006.

[59] Stern M, Catelani G, Kubo Y, et al[J]. 2014 Phys. Rev. Lett. 113 123601.

[60] Orgiazzi J L, Deng C, Layden D, et al[J]. 2016 Phys. Rev. B 93 104518.

[61] Yu H F, Zhu X B, Peng Z H, et al[J]. 2010 Phys. Rev. B 81 144518.

[62] Yu H F, Zhu X B, Ren J K, et al[J].2013 New J. Phys. 15 095006.

[63] Li S X, Qiu W, Han S, et al[J]. 2007 Phys. Rev. Lett. 99 037002.

[64] Yu H F, Zhu X B, Peng Z H, et al[J]. 2011 Phys. Rev. Lett. 107 067004.

[65] Xue G M, Gong M, Xu H K, et al[J]. 2014 Phys. Rev. B 90 224505.

[66] Roushan P, Neill C, Chen Yu, et al[J]. 2014 Nature 515 241.

[67] Wang C, Gao Y Y, Reinhold P, et al[J]. 2016 Science 352 1087

[68] Baur M, Filipp S, Bianchetti R, et al[J]. 2009 Phys. Rev. Lett. 102 243602.

[69] Novikov S, Robinson J E, Keane Z K, S et al[J]. 2013 Phys. Rev. B 88 060503.

[70] Suri B, Keane Z K, Ruskov R, et al.2013 New J. Phys. 15 125007.

[71] Novikov S, Sweeney T, Robinson J E, et al[J]. 2016 Nat. Phys. 12 75.

[72] Liu Q C, Li T F, Luo X Q, et al[J]. 2016 Phys. Rev. A 93 053838.

[73] Astafiev O, Zagoskin A M, Abdumalikov Jr. A A, et al[J]. 2010 Science 327 840.

[74] Peng Z H, Liu Y X, Peltonen J T, et al[J]. 2015 Phys. Rev. Lett. 115 223603.

[75] Feynman. R Simulating physics with computers[J]. International Journal of Theoretical Physics 21, 467–488 (1982).

[76] Shor. P. W. Algorithms for quantum computation: discrete logarithms and factoring[J]. In Symposium on Foundations of Computer Science, 124–134 (1994).

[77] Grover. L. K A fast quantum mechanical algorithm for database search[J]. In Twenty-Eighth ACM Symposium on Theory of Computing, 212–219 (1996).

[78] Monroe. C., Meekhof. D. M, King. B. E, et al. Demonstration of a fundamental quantum logic gate[J]. Phys. Rev. Lett. 75, 4714–4717 (1995).

[79] Cirac. J. I, Zoller. P Quantum computations with cold trapped ions[J]. Phys. Rev. Lett. 74, 4091–4094 (1995).

[80] Knill. E, Laflamme. R, Milburn. G. J A scheme for efficient quantum computation with linear optics[J]. Nature 409, 46 (2001).

[81] Rossetti. R, Nakahara. S, Brus. L. E Quantum size effects in the redox potentials, resonance raman spectra, and electronic spectra of cds crystallites in aqueous solution[J]. Journal of Chemical Physics 79, 1086–1088 (1983).

[82] Gershenfeld. N. A, Chuang. I. L Bulk spin-resonance quantum computation[J]. Science 275, 350–356 (1997).

[83] Byrnes. T , Wen K , Yamamoto. Y. Macroscopic quantum computation using bose-einstein condensates[J]. Phys. Rev. A 85, 040306 (2012).

[84] Childress. L, et al. Coherent dynamics of coupled electron and nuclear spin qubits in diamond[J]. Science 314, 281–285 (2006).

[85] Wendin G. Quantum information processing with superconducting circuits: a review [J]. Rep Prog Phys, 2017, 80(10): 106001.

Special Column: Superconducting Quantum Computing and Engineering

Superconducting quantum bits (qubits) and circuits are the leading candidates for the implementation of solid-state quantum computation. This column will discuss superconducting quantum computing in physical principle, measurement, fabrication, and experimental examples.